JOURNAL OF COMPUTATIONAL PHYSICS 60, 549–557 (1985)

Comments on the Stability of the RSF Three-Dimensional MHD Plasma Simulation Algorithm

J. W. EASTWOOD AND K. I. HOPCRAFT*

Theoretical Physics Division, Culham Laboratory, Abingdon, Oxon, OX14, 3DB, England

Received September 26, 1983; revised August 15, 1984

1. INTRODUCTION

RSF [1] is a spectral code which follows the time evolution of the reduced MHD equations [2]. Its numerical results have been central to much development of the theory of nonlinear tearing modes and disruptions in tokamaks [2, 3, and references therein]. RSF has shown quantitatively different behaviour of plasma variables as magnetic Lundquist numbers are raised to values ($S \sim 10^6$) which are beyond the capabilities of existing finite difference codes.

The purpose of this note is to discuss the stability properties of the time integration scheme used in RSF. The consequences of its weak stability properties are that (i) unnecessarily small timesteps Δt may be needed, (ii) physical processes may become confused with numerical effects, and (iii) the code may catastrophically fail. Code failure may be due either to exponential growth causing overflow, or in the case of adaptive timesteps, the timestep becoming exponentially small. If the timestep becoming too small is the only difficulty, then it is still of importance to understand why this occurs in order to devise more efficient schemes to bring physical parameters encountered in tokamaks within the capability of present day computers. If physical processes are modified, the whole of the computations becomes open to question.

We show in this note for both the typographically incorrect published algorithm [1] and for the corrected algorithm [7] that stability of the integration scheme relies on the coupling of the flux and vorticity equation: The vorticity advection scheme is of the centred space/forward time type which requires the addition of physical or numerical dissipation for stability. For the inviscid plasma model used in RSF, stabilisation requires $\mathbf{K} \cdot \mathbf{B}$ nonzero (cf. below), so for zero magnetic field or wavenumber function $\mathbf{K}$ perpendicular to $\mathbf{B}$, the scheme is unconditionally unstable. The published stability criterion given for RSF is necessary, but not sufficient. For large S and for nonzero plasma flow, much more stringent conditions must be satisfied.

* Present address: Blackett Laboratory, Imperial College, London SW7, England.

0021-9991/85 $3.00

2. Model Equations

The large aspect ratio limit orders toroidal curvature out of the equations. Consequently, the reduced equations may be written in polar (r, θ, z) or cartesian (x, y, z) coordinates with z corresponding to the toroidal direction as:

$$\frac{\partial U}{\partial t} = -\mathbf{v}\cdot\nabla U - S^2\left(\mathbf{e}_z\times\nabla\psi\cdot\nabla j + \frac{\partial j}{\partial z}\right) \tag{1}$$

$$\frac{\partial \psi}{\partial t} = -E_z^w - \mathbf{B}\cdot\nabla\phi + \eta j \tag{2}$$

$$\mathbf{v} = \nabla\phi\times\mathbf{e}_z \tag{3}$$

$$j = \nabla_\perp^2\psi \tag{4}$$

$$U = \nabla_\perp^2\phi. \tag{5}$$

The definition of variables and operators follows [1]. $\mathbf{e}_z$ is the unit vector in the z direction. With appropriate choice of z scale length, the magnetic field is related to the flux function, ψ, by

$$\mathbf{B} = \mathbf{e}_z\times\nabla\psi + \mathbf{e}_z.$$

Equations (1)–(5) describe an incompressible magnetofluid where poloidal currents and toroidal magnetic field variations are negligible. Energy flows into the system through the wall Poynting flux, is stored in magnetic and bulk flow energy, and flows out by ohmic dissipation. The model equations describe Alfvén waves and tearing modes.

A dispersion relation may be obtained by linearising Eqs. (1)–(5) about a uniform slab equilibrium in cartesian coordinates with $\eta = 1$, $j_0 = U_0 = 0$, $\mathbf{B}_0 = \text{constant}$, $\mathbf{v}_0 = 0$, and taking a disturbance $\sim\exp[-i(\omega t - \mathbf{k}\cdot\mathbf{x})]$:

$$\begin{aligned} \omega_r^2 &= S^2(\mathbf{k}\cdot\mathbf{B}_0)^2 - \left(\frac{k_\perp^2}{2}\right)^2, && \omega_r^2 > 0, \\ &= 0 && \text{otherwise} \end{aligned} \tag{6}$$

$$\begin{aligned} \omega_i &= -\frac{k_\perp^2}{2}, && \omega_r^2 > 0, \\ &= -\frac{k_\perp^2}{2} \pm \left[\left(\frac{k_\perp^2}{2}\right)^2 - S^2(\mathbf{k}\cdot\mathbf{B}_0)^2\right]^{1/2} && \text{otherwise.} \end{aligned} \tag{7}$$

Equations (6)–(7) differ from the MHD results only in that k^2 is replaced by its projection $k_\perp^2$ on the poloidal plane. The modification of the Alfvén wave eigenfrequencies by the space–time lattice is the source of the numerical instabilities listed in Section 1.

3. Discrete Approximation

Equations (1)–(5) are discretised in polar coordinates (r, θ, z) in RSF by using a Galerkin method on a set of helical trial functions $\sim \exp i[m\theta + nz]$, second-order finite differences to treat radial derivatives and a two step second-order accurate time discretisation to deal with time derivatives [1, 7].

The algebraic equations to be solved in advancing the system from time t to time $t + \Delta t$ are

$$U^{t+\Delta t/2} = U^t + \frac{\Delta t}{2} S_u^t \tag{8}$$

$$\psi^{t+\Delta t/2} = \psi^t + \frac{\Delta t}{2}(\eta j^{t+\Delta t/2} - E_z^w - \mathbf{B}_a \cdot \nabla \phi^{t+\Delta t/2}) - \frac{\Delta t}{2} \delta \mathbf{B}^t \cdot \nabla \phi^t \tag{9}$$

$$U^{t+\Delta t} = U^t + \Delta t\, S_u^{t+\Delta t/2} \tag{10}$$

$$\psi^{t+\Delta t} = \psi^t + \Delta t\, S_\psi^{t+\Delta/2} \tag{11}$$

where S_u and S_ψ are the right-hand sides of Eqs. (1) and (2) with derivatives replaced by their Fourier mode/finite difference approximations. Implicit treatment of the Ohmic dissipation in Eq. (9) has a stabilizing effect which offsets partially the destabilising influence of explicit advection terms. In the typographically incorrect algorithm [1], $\mathbf{B}_a = 0$ and $\delta \mathbf{B} = \mathbf{B}$, whilst in the correct algorithm [7], $\mathbf{B}_a$ is the initial axisymmetric field and $\delta \mathbf{B} = \mathbf{B} - \mathbf{B}_a$. This change improves the numerical stability.

4. Stability Analysis

To investigate the linear stability properties of the discrete algebraic plasma model, we consider a uniform magnetised plasma in slab geometry. We take a mesh in the y direction and fourier modes in the x and z directions. This may be viewed as a local (short wavelength) approximation to the cylindrical geometry, where r, θ, and z map respectively to y, x, and z. We implicitly assume that the high frequency Alfvén modes are the limiting factor on the time integration: the analysis does not include current gradients, mesh, and field curvature. If the scheme proves inadequate even in the simplest situations, it is unlikely to be stabilised when extra physically destabilising effects are included.

Equilibria are defined by selecting U_0, $\mathbf{B}_0$, j_0, ϕ, such that $S_u^0 = S_\psi^0 = 0$. Again, the local nature of the analysis should be borne in mind: If $\mathbf{B}_0$ corresponds to the $(m, n) = (0, 0)$ mode at time $t = 0$, then the whole of the $\mathbf{B} \cdot \nabla \phi$ term in Eq. (9) should be treated as implicit. At later times, as the axisymmetric part evolves, the term becomes partly implicit, partly explicit. For $(m, n) \neq (0, 0)$, all contributions to $\mathbf{B} \cdot \nabla \phi$ term are explicit. Since the stability analysis is concerned with limiting cases,

we take the worst case where the $\mathbf{B}\cdot\nabla\phi$ term is explicit: This is pessimistic for early stages of a calculation where the field is predominantly the implicit part of the (0, 0) mode, but not so for later stages.

Dispersion and stability are analysed in the same manner as for the continuum case: Fourier analysing the linearised forms of Eqs. (8)–(11) and eliminating reference to the half timelevels gives an equation of the form

$$\begin{bmatrix}\tilde{U}\\ \tilde{\psi}\end{bmatrix}^{t+\Delta t} = \mathbf{\Lambda}(\mathbf{k})\begin{bmatrix}\tilde{U}\\ \tilde{\psi}\end{bmatrix}^{t} \tag{12}$$

for the perturbed variables $\tilde{U}$, $\tilde{\psi}$. The amplification matrix $\mathbf{\Lambda}$ must have eigenvalues in the unit circle for stability [4, Chap. 4]. The dispersion relation for the numerical plasma model is

$$\det(\mathbf{\Lambda}-\lambda\mathbf{1})=0 \tag{13}$$

where $\lambda=\exp[-i\omega\Delta t]$.

Solving Eq. (13) for the case where the plasma is at rest in the mesh frame of reference gives

$$\lambda=\frac{[1-2g^2(1+ag)\pm 2g[a^2(g^2+1)^2-1]^{1/2}]}{(1+2ag)} \tag{14}$$

where

$$g=S(\mathbf{K}\cdot\mathbf{B}_0)\frac{\Delta t}{2}; \qquad a=\frac{\kappa_\perp^2/2}{S(\mathbf{K}\cdot\mathbf{B}_0)}$$

and $\mathbf{K}$ and $\kappa_\perp^2$ are the Fourier transforms of the discretised ∇ and $\nabla_\perp^2$ operators, respectively.

In the limit $\Delta t\to 0$, Eq. (14) reduces to equations of the form of Eqs. (6) and (7), differing only in that $\mathbf{k}$ and $k_\perp^2$ are replaced by the spatial finite difference modified forms $\mathbf{K}$ and $\kappa_\perp^2$. For finite Δt, the numerical approximation to Alfvén waves given by Eq. (14) describes damped waves, provided that $|\lambda|<1$. Hence, numerically stable timesteps are those for which $|\lambda|\leqslant 1$. Finite Δt errors are negligible when solutions of Eq. (14) deviate only slightly from those of Eqs. (6) and (7), i.e., when $i\omega'+(\lambda-1)/\Delta t$ is small, where ω' is given by Eqs. (6) and (7).

4.1. $S\to\infty$ *Limit*

In the limit $S\to\infty$, with $S\Delta t=$ constant (i.e., timestep is fixed in Alfvén time units, so g remains finite and $a\to 0$) Eq. (14) reduces to $\lambda=1-2g^2\pm i2g$, giving

$$|\lambda|=[1+4g^4]^{1/2}>1 \qquad \text{for } g\neq 0,$$

i.e., the algorithm is unconditionally unstable for $S\to\infty$.

4.2. *Finite S, Zero Flow*

The curve $a(g^2+1)=1$ divides the g/a parameter space into regions where λ is real (evanscent roots) and λ is complex (oscillatory roots). Substituting Eq. (14) into $|\lambda|^2<1$ gives the stability limit in the two instances:

$$\begin{aligned} -g^4+2ag^3+g^2-1 &\leqslant 0, \qquad \lambda \text{ real} \\ g^3-ag^2-a &\leqslant 0, \qquad \lambda \text{ complex} \end{aligned} \tag{15}$$

The published stability criterion [1]

$$S \max \left| \frac{m}{q} - n \right| \frac{\Delta t}{2} \leqslant 1 \tag{16}$$

is a singular result, as it only applies for the initial axisymmetric field and for zero flow. For small changes from the initial equilibrium, the stability criterion *in the absence of flow* becomes

$$g \simeq S \max / k_r B_r + \frac{m}{q} - n \left| \frac{\Delta t}{2} \leqslant 1, \right. \tag{17}$$

where $k_r \sim \pi/2\Delta r$. Equation (17) reduces to Eq. (16) only when island widths are small compared to mesh spacings. Thus the suggestion in [1] that Δt is independent of grid spacing is somewhat misleading.

For large S, stability for the arbitrary field orientation is determined by the second case in Eq. (15); this is because the wavenumber at which Alfvén waves become evanescent is larger than the largest wavenumber resolved on the radial mesh at large S. A sufficiency condition arising from Eq. (15) for λ complex is

$$g \leqslant a^{1/3} \{ \leqslant [a(1+g^2)]^{1/3} \} \tag{18}$$

provided that the flow velocity $\mathbf{v}$ is zero. *Thus, the algorithm becomes increasingly unstable at large S, and the criterion Eq.* (16) *is necessary but not sufficient.*

4.3. *Non-zero Flow*, $\mathbf{K} \cdot \mathbf{B}_0 = 0$

Non-zero flow does not simply mean Doppler-shift frequencies as in the continuum case. It allows the possibility of further instabilities. Extending Eq. (14) to include uniform flow $\mathbf{v}_0$ is straightforward but tedious. For the special case $\mathbf{K} \cdot \mathbf{B}_0 = 0$, the vorticity ($U$) and flux ($\psi$) equations decouple, and the vorticity equation gives the stability criterion

$$1 + 4 \left[(\mathbf{K} \cdot \mathbf{v}_0) \frac{\Delta t}{2} \right]^4 \leqslant 1, \tag{19}$$

i.e., *the scheme is unconditionally unstable for flows with wavenumbers such that* $\mathbf{K} \cdot \mathbf{B}_0 = 0$.

4.4. *General Case*

The most general case we consider is the stability of Alfvén waves for arbitrary flow velocity and magnetic field orientation w.r.t. the radial mesh. This may be interpreted as a local (short wavelength) analysis applicable when large island structures are established. Following the procedure of Eqs. (12)–(14) yields a complex quadratic for λ when flow velocity $\mathbf{v}$ is nonzero. Solving numerically for the marginally stable waves $|\lambda| = 1$ gives Fig. 1. Figure 1 summarises the regions of the g–c plane for stable operation for a range of flow velocity parameters d, where

$$c = (\kappa_\perp^2/2)(\Delta t/2), \qquad d = (\mathbf{K} \cdot \mathbf{v})(\Delta t/2).$$

The figure may be interpreted as a projection of a 3-dimensional volume in g–c–d space within which operating points of the time integration scheme are stable. Parameters g, c, d respectively give the ratio of timestep to characteristic timescales for Alfvén waves, resistive decay, and flow.

The stability volume is that part of g, c, d space, where $|\lambda| \leqslant 1$. Stability criteria for integration schemes are generally obtained by defining some volume around the origin which is enclosed by the stability volume, i.e., one tries to establish an expression of the form $\max\{\alpha\,|g| + \beta\,|c| + \gamma\,|d|\} \leqslant 1$. Since the stability volume

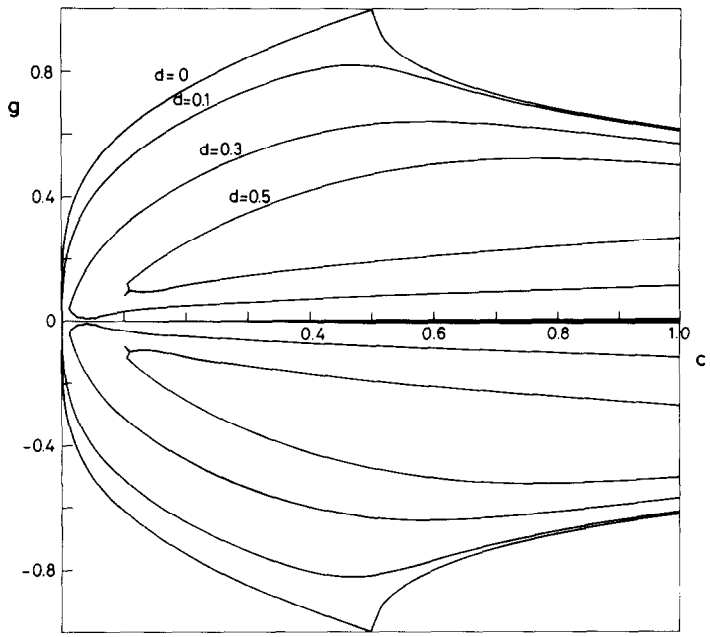

FIG. 1. Stability boundaries in the g–c plane for a range of values of d. Parameters g, c, d are respectively ratios of the timestep to characteristic Alfvén, resistive decay, and flow transit times, (see text). The stable regions shrink with increasing d.

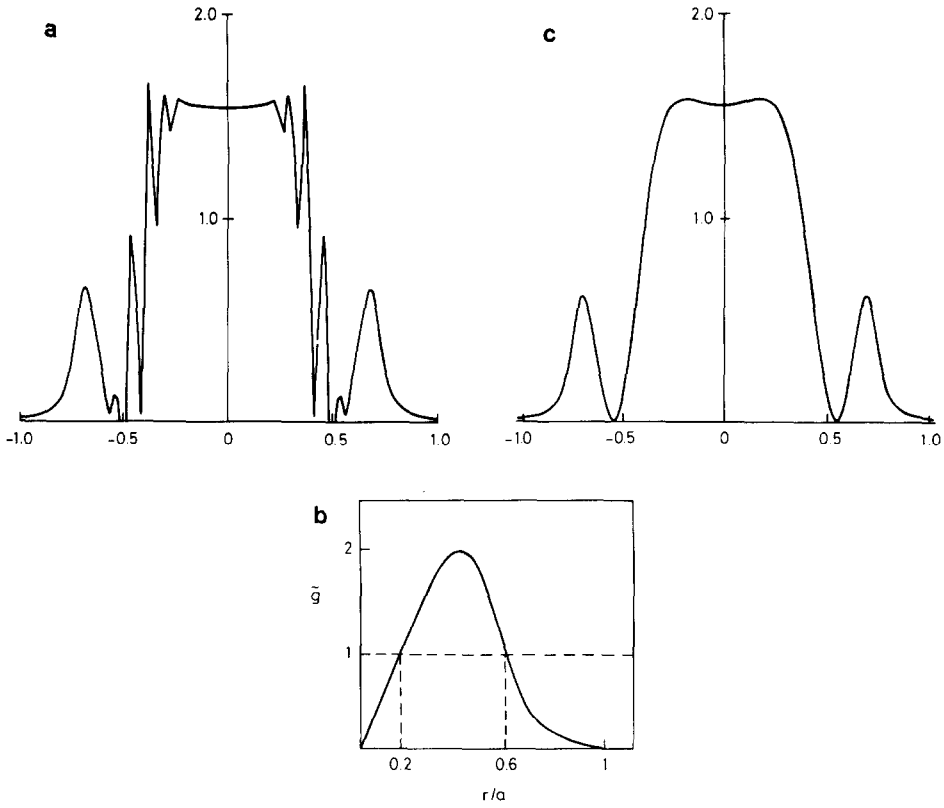

FIG. 2. (a) Current density profile versus minor radius at step 114, $t = 2.17 \times 10^{-2}\tau_R$; (b) Stability parameter versus minor radius at step 114; (c) Current density profile at step 750, $t = 2.41 \times 10^{-2}\tau_R$. The timestep is set such that $\tilde{g} < 1$.

has clefts reaching the origin around the $c = 0$ (large S) and $g = 0$ (small $\mathbf{K} \cdot \mathbf{B}$) planes, an easily computable stability criterion is difficult to define. Indeed, the above bounding methods (cf. Sect. 4.3) give unconditional instability as the result!

5. COMPUTATIONAL RESULTS

Figure 2 illustrates timestepping instability in a single mode calculation ($m = 2$, $n = 1$). We have used a copy of the program RSF provided by Hicks [6]. The flat top current profile defined in [3, Eq. (21)] with ($q_l = 4.2$, $q(0) = 1.34$, $\lambda = 3.24$) was used as initial conditions, and the nonlinear evolution was followed using RSF with $N_g = 100$ radial grid points, and an initial timestep $\Delta t = 0.8$ times the stability limit value in the initial axisymmetric field.

Figure 2a shows the current density profile at step 114. The peak between

$r/a = 0.6$–0.8 corresponds to the 2/1 island, and the spikes between $r/a = 0.2$–0.6 are numerical. Note that the width of the spikes is large compared to the mesh spacing, as is predicted by the stability analysis. Figure 2b shows an estimator $\tilde{g}$ of the stability parameter g:

$$\tilde{g} = \frac{S}{2\Delta t}\left[\frac{\pi N_g}{2}\max\left|\frac{m\tilde{\psi}_{mn(r)}}{r}\right| + \max\left|\frac{m}{q} - n\right|\right]$$

computed at the same timestep as Fig. 2a. Appearance of instability correlates well with $\tilde{g} > 1$. Reducing the timestep to ensure $\tilde{g} < 1$ leads to the smooth final state shown in Fig. 2c.

The stability criterion $g \simeq \tilde{g} < 1$ is good only when changes from the initial field is small and flow is such that $g \gg d$; $\tilde{g} < 1$ is a necessary condition for stability, but not sufficient. These calculations are presented to illustrate the instability mechanism, not the stability bound. To have a sharp stability bound, the integration scheme must be modified [5].

6. Final Remarks

The stability of the published RSF algorithms [1, 7] depend on timestep, radial mesh spacing, allowed modes, magnetic field configuration, and flow velocity. Clearly it is possible to initiate computations which are numerically stable, but it is difficult to assure stability through the nonlinear evolution of fields and flow, particularly for large S.

Conventional bounding techniques on numerical algorithms seek criteria of the form $|v|\,\Delta t/\Delta x < \alpha$ where α is some number. Analysis presented here shows that such a criterion does not hold for the scheme considered here. Additional dissipation or orientational information ($\mathbf{K} \cdot \mathbf{B} \neq 0$) is needed to eliminate the possibility of flow driven instabilities. Alfvén wave damping is reduced to marginal levels when $g \sim a^{1/3}$ if S is large. Since Alfvén waves are an important means of transporting energy from disturbances at large S, numerical destabilisation can have significant effects.

To avoid confusing numerical and physical effects in computational results it is desirable to employ a more stable algorithm. Also it is essential to (i) perform convergence checks, (ii) monitor linear stability, and (iii) maintain running checks on energy conservation. Points (i) and (iii) are discussed in [1]. We shall present further details of these points, together with discussions of nonlinear interaction with the timestep reduction algorithm, of spatial aliasing, and of algorithm improvements in future reports [5]. If large S values are necessary, then such computations will continue to demand more efficient algorithms and more powerful computers.

ACKNOWLEDGMENTS

The work reported here was stimulated by the interests of Dr. J. A. Wesson of the JET Joint Undertaking. We also extend our thanks to H. R. Hicks for providing a copy of the RSF program and for giving helpful advice on running the program.

REFERENCES

1. H. R. HICKS, B. CARRERAS, J. A. HOLMES, D. K. LEE, AND B. V. WADDELL, *J. Comput. Phys.* **44** (1981), 46–69.
2. B. V. WADDELL, B. CARRERAS, H. R. HICKS, AND J. A. HOLMES, *Phys. Fluids* **22** (1979), 896–910.
3. B. CARRERAS, H. R. HICKS, J. A. HOLMES, AND B. V. WADDELL, *Phys. Fluids* **23** (1980), 1811–1826.
4. R. W. HOCKNEY AND J. W. EASTWOOD, "Computer Simulation Using Particles," McGraw–Hill, New York, 1981.
5. in preparation.
6. H. R. HICKS, private communication, 1983.
7. H. R. HICKS, B. CARRERAS, J. A. HOLMES, D. K. LEE, AND B. V. WADDELL, *J. Comput. Phys.* **53** (1984), 205.